RAMAN, INFRARED, AND NEAR-INFRARED CHEMICAL IMAGING

EDITED BY

SLOBODAN ŠAŠIĆ
YUKIHIRO OZAKI

WILEY

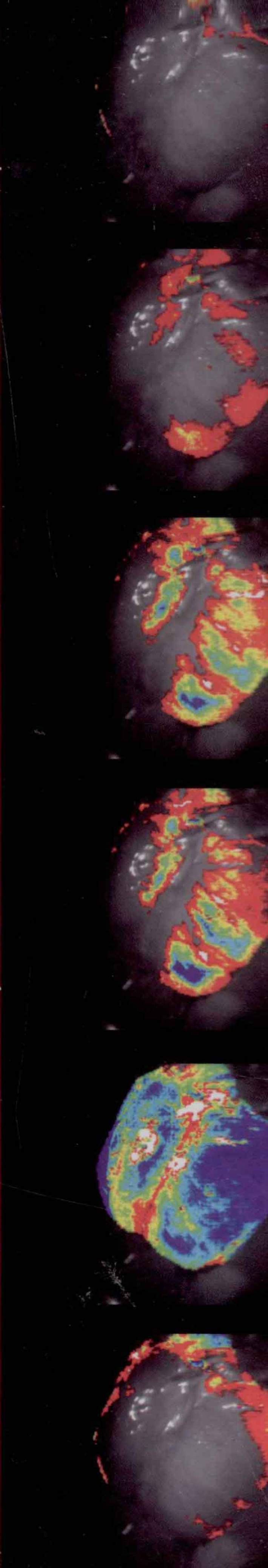

RAMAN, INFRARED, AND NEAR-INFRARED CHEMICAL IMAGING

Edited by

SLOBODAN ŠAŠIĆ
Pfizer
Groton, Connecticut, USA

YUKIHIRO OZAKI
Kwansei Gakuin University
Sanda, Japan

WILEY
A JOHN WILEY & SONS, INC., PUBLICATION

Published by John Wiley & Sons, Inc., Hoboken, New Jersey
Published simultaneously in Canada

Library of Congress Cataloging-in-Publication Data:

Raman, infrared, and near-infrared chemical imaging / edited by Slobodan Šašić, Yukihiro Ozaki.
p. cm.
Includes index.
ISBN 978-0-470-38204-2 (cloth)
1. Raman spectroscopy. 2. Infrared imaging. 3. Imaging systems in chemistry. I. Šašić, Slobodan. II. Ozaki, Y. (Yukihiro)
QD96.R34R36 2011
543′.57–dc22

2010010781

Printed in the United States of America

10 9 8 7 6 5 4 3 2 1

PREFACE

Vibrational spectroscopy-based chemical imaging is a comparatively new imaging approach that has become truly operational in the past 10 years. It applies to samples more frequently met in academic rather than industrial laboratories, and it is used for exploration rather than routine analysis. However, it is steadily improving, gaining recognition in various industries, and finding use for solving a variety of real-world problems. The key points of chemical imaging based on Raman, infrared, or near-infrared response/spectra are chemical specificity and richness of information that stems from the collection of full-range spectra. Such wealth of data is usually best handled by the linear algebra-based algorithms that have once been considered fairly advanced but today are much more of a commonplace among this chemical imaging community. Applications of linear algebra (known as chemometrics in this field) are possible due to the assumed linearity of the responses from the imaged sample. Thus, quite often, a chemical imaging application (in this context) is a nice example of usefulness of chemometrics for extracting the information that would normally be unattainable or ambiguous by simply following response at a wavenumber that is considered indicative of a sought component (which, in fact, is the most commonly followed approach in the broadly popular imaging techniques). Many cases depicted in this book necessitate chemometrics for obtaining meaningful images.

Hardware is another key element in the development of chemical imaging. The improvement in combining spectrometers with microscopes (which roughly stands for a chemical imaging instrument) has been tremendous in recent times and certainly hugely contributed to this type of chemical imaging to become more widely used. It may not be an exaggeration to say that at present it is the applications that are somewhat behind what technically can be obtained from the available instruments. In this book, particular attention is paid to hardware.

The same holds for software. There are a couple of commercial software to chose from, and users quite frequently individually employ programming languages (with Matlab being unquestionably predominant) to tackle these complex 3D (or 4D) data sets via routines that do not really involve much more than skillfully combining existing algorithms. Here, it is not so much about improving the computational approaches as many of them have been used quite broadly for diverse problems, but rather finding suitable applications in this imaging field to demonstrate the ability to extract reliable information buried somewhere among thousands of spectra with hundreds of data points.

This book tries to portray all facets of chemical imaging via vibrational spectra. It starts with introducing vibrational spectroscopy, addresses hardware in more and software in less details (due to frequent references to computational details in the applications), and then methodically lists applications in several fields of which the biomedical and pharmaceutical ones probably dominate as for the number and impact of the publications, followed by no less promising and important food and polymers. A glimpse into future is also taken by listing several cutting-edge experimental endeavors. Each of the chapters in the book aims at covering all the three vibrational spectroscopy mechanisms (Raman, IR, and NIR) with Raman being given some more attention in the closing chapters. While, in essence, producing a chemical image may not be a tough task and can be done easily in some cases, it takes an expert with substantial knowledge of spectroscopy and chemometrics to single-handedly tackle demanding cases and unravel useful information from the labyrinth of data intrinsic to such experiments. The editors believe that the authors of this book are such individuals, world-class scientists, and authorities in respective fields. We hope that the joint effort presented in this book is an influential source of information on what chemical imaging is, how and what for to use it, and where to look for additional information. We hope readers will enjoy reading it as much as the authors enjoyed writing.

February 2010

Slobodan Šašić and Yukihiro Ozaki

CONTRIBUTORS

Nils Kristian Afseth, Nofima Mat As, Ås, Norway

Ulrike Böcker, Nofima Mat As, Ås, Norway

R. A. Crocombe, Thermo Fischer Scientific, Billerica, MA, USA

Janie Dubois, Malvern Instruments, Columbia, MD, USA

Carol R. Flach, Department of Chemistry, Newark College, Rutgers University, Newark, NJ, USA

Paul Geladi, Unit of Biomass Technology and Chemistry, Swedish University of Agricultural Sciences, Umeå, Sweden

Ad Gerich, Schering Plough, Oss, The Netherlands

Hans Grahn, Department of Neuroscience, Division of Behavioral Neuroscience, Karolinska Institute, Stockholm, Sweden

Hiro-o Hamaguchi, Department of Chemistry, School of Science, The University of Tokyo, Tokyo, Japan

Xiaoxia Han, State Key Laboratory of Supramolecular Structure and Materials, Jilin University, Changchun, China

Mohammad Kamal Hossain, Department of Chemistry, School of Science and Technology, Kwansei Gakuin University, Sanda, Japan

R. A. Hoult, PerkinElmer, Buckinghamshire, UK

Yu-San Huang, Department of Chemistry, School of Science, The University of Tokyo, Tokyo, Japan

Tamitake Itoh, National Institute of Advanced Industrial Science and Technology, Takamatsu, Kagawa, Japan

Jianhui Jiang, State Key Laboratory of Chemo/Biosensing and Chemometrics, Hunan University, Changsha, China

Olga Jilkina, Institute for Biodiagnostics, National Research Council of Canada, Winnipeg, Manitoba, Canada

Hideaki Kano, Department of Chemistry, School of Science, The University of Tokyo, Tokyo, Japan; PRESTO (Precursory Research for Embryonic Science and Technology), Japan Science and Technology Agency, Saitama, Japan

Yasutaka Kitahama, Department of Chemistry, School of Science and Technology, Kwansei Gakuin University, Sanda, Japan

Sergei G. Kazarian, Department of Chemical Engineering, Imperial College London, London, UK

Linda H. Kidder, Malvern Instruments, Columbia, MD, USA

Valery V. Kupriyanov, Institute for Biodiagnostics, National Research Council of Canada, Winnipeg, Manitoba, Canada

E. Neil Lewis, Malvern Instruments, Columbia, MD, USA

Gurjit S. Mandair, Department of Chemistry, University of Michigan, Ann Arbor, MI, USA

Marena Manley, Department of Food Science, Stellenbosch University, Stellenbosch, South Africa

Richard Mendelsohn, Department of Chemistry, Newark College, Rutgers University Newark, NJ, USA

David J. Moore, ISP Corporation, Wayne, NJ, USA

Michael D. Morris, Department of Chemistry, University of Michigan, Ann Arbor, MI, USA

Yasuaki Naito, Department of Chemistry, Gakushuin University, Tokyo, Japan

Matthew P. Nelson, ChemImage Corporation, Pittsburgh, PA, USA

Yukihiro Ozaki, Department of Chemistry, School of Science and Technology, Kwansei Gakuin University, Sanda, Japan

C. C. Pelletier, NASA-Jet Propulsion Laboratory, Gales Ferry, CT, USA

M. J. Pelletier, Pfizer, Groton, CT, USA

Slobodan Šašić, Analytical Development, Pfizer, Groton, CT, USA

Harumi Sato, Department of Chemistry, School of Science and Technology, Kwansei Gakuin University, Sanda, Japan

J. Sellors, PerkinElmer, Buckinghamshire, UK

Laurence Senak, ISP Corporation, Wayne, NJ, USA

R. Anthony Shaw, Institute for Biodiagnostics, National Research Council of Canada, Winnipeg, Manitoba, Canada

Rintaro Shimada, Department of Chemistry, School of Science, The University of Tokyo, Tokyo, Japan

Hideyuki Shinzawa, Research Institute of Instrumentation Frontier, Advanced Industrial Science and Technology (AIST), Chubu, Nagoya, Japan

Michael G. Sowa, Institute for Biodiagnostics, National Research Council of Canada, Winnipeg, Manitoba, Canada

Athiyanathil Sujith, National Institute of Technology Calicut, Calicut, Kerala, India

Patrick J. Treado, ChemImage Corporation, Pittsburgh, PA, USA

Patrick S. Wray, Department of Chemical Engineering, Imperial College London, London, UK

N. A. Wright, Applied Instrument Technologies, Hamilton Sundstrand, Pomona, CA, USA

Ru-Qin Yu, State Key Laboratory of Chemo/Biosensing and Chemometrics, Hunan University, Changsha, China

Lin Zhang, Analytical Development, Pfizer, Groton, CT, USA

CONTENTS

1

SPECTROSCOPIC THEORY FOR CHEMICAL IMAGING

M. J. PELLETIER
Pfizer, Groton, CT, USA
C. C. PELLETIER[1]
NASA–Jet Propulsion Laboratory, Gales Ferry, CT, USA

1.1 INTRODUCTION

All images require some type of contrast to differentiate regions of interest in a field of view. The most common source of image contrast is variation in the intensity of reflected light. Contrast can, however, be based upon any measurable property of the sample that can be expressed as a function of location. Contrast is improved for measurements having a wider dynamic range and by measuring a larger number of variables for each pixel, as in color versus black-and-white photography. Contrast may also be enhanced with one or more of a wide range of techniques including digital image processing and structured illumination. This book will focus on chemical images generated using vibrational spectroscopic contrast. Such contrast is generated by quantifying one or more attribute(s) of an infrared absorption, infrared emission, or Raman scattering spectrum for each pixel. By providing a window into the spatial distribution of properties such as molecular composition, structure, state, and concentration, images based on vibrational spectroscopies open up a new way of seeing the world.

Imaging can be accomplished by measuring a property from the entire field of view simultaneously (global imaging) or by measuring a property from individual points in the field of view sequentially and combining the points to create the image (mapping). Since mapping requires a large number of measurements, each measurement must be relatively fast for mapping to be practical. For example, an image consisting of 640×480 pixels contains over 300,000 measurements and would take more than 3.5 days to acquire if each measurement required 1 s. Mapping speed can be increased by simultaneously measuring a property at multiple points in a subregion of the field of view and combining those subregions to create the image. The subregion may consist of a single column of measurement points (line imaging) or may contain multiple columns (mosaic imaging). In most cases, even global imaging requires multiple frames, each containing different spectroscopic information, to be collected sequentially and overlaid to form a single image. Sample changes during the course of sequential measurements can confound the interpretation of spectral images.

This chapter provides an introduction and theoretical background for vibrational spectroscopies, as used to produce chemical images. Infrared, Raman, and related spectra result from the interactions of electromagnetic radiation with molecular vibrations, so this chapter begins with a description of relevant aspects of molecular vibration, followed by a section on electromagnetic radiation and its interactions with matter. Next are three sections on infrared spectroscopies, divided by spectral region. After that, several different types of Raman spectroscopy that are used for chemical imaging are described. The final section briefly presents the use of Raman and infrared spectroscopies for creating large chemical images by remote sensing. Remote sensing is probably responsible for the majority of chemical images created because of its use in mapping the atmosphere, planets including Earth, and moons, and in astronomy.

[1] Retired

Raman, Infrared, and Near-Infrared Chemical Imaging Edited by Slobodan Šašić and Yukihiro Ozaki

1.2 MOLECULAR VIBRATIONS

A chemical bond between two atoms can be modeled as a spring connecting two point masses. If the spring follows Hook's law, the force it applies between the two point masses will be proportional to the spring displacement from its lowest energy position. The system, called a harmonic oscillator, will have a single resonant vibrational frequency, υ, given by

$$\upsilon = \frac{1}{2\pi c}\left(\frac{k}{\mu}\right)^{1/2} \tag{1.1}$$

where c is the speed of light, k is the force constant, and μ is the reduced mass, $m_a m_b/(m_a + m_b)$.

Equation 1.1 describes the vibrational frequency of diatomic molecules reasonably well. Increasing the strength of the chemical bond increases the vibrational frequency. Increasing the atomic mass reduces the vibrational frequency.

The force applied by a chemical bond does not follow Hook's law exactly, though. Atoms have finite size and cannot occupy the same space. As a result, the repulsive force increases much more quickly than Hook's law would predict as the atoms get close together. As the atoms get further apart the chemical bond weakens, approaching zero strength at infinite separation, again violating Hook's law. Deviations from Hook's law are amplified by disparity between the molecular masses. Vibrating systems that do not follow Hook's law are called anharmonic, and the extent to which they deviate from an ideal harmonic oscillator is called anharmonicity. Anharmonicity has a relatively small role in most forms of Raman spectroscopy, a somewhat larger role in mid-infrared (mid-IR) spectroscopy, and is of primary importance in near-infrared (NIR) spectroscopy.

Vibrations in molecules containing more than two atoms are more complicated. The total number of different, or normal, vibrations (ignoring anharmonicity) in a molecule with n atoms is $3n - 5$ for a linear molecule and $3n - 6$ for a nonlinear molecule. For example, an anthracene molecule has 24 atoms and therefore 66 normal vibrations. Some of these vibrations have exactly the same frequency (called degenerate vibrations). Other vibrations produce no signal for a particular type of vibrational spectroscopy due to symmetry constraints. As a result of these spectral simplifications, even most large molecules have manageable vibrational spectra.

Oscillators sharing a common atom may exert forces on each other when they oscillate. If the oscillator frequencies are very different from each other, each oscillator remains fairly independent of the other. If the frequencies are similar, though, the oscillators can couple, essentially forming a new single oscillator with new frequencies. Consider the linear CO_2 molecule. Both carbon–oxygen bonds are identical. They couple to form a single oscillator having two different vibrations. One vibration consists of each carbon–oxygen bond stretching in phase, resulting in a vibration where the carbon atom does not move. This in-phase vibration is an example of a symmetric vibration. The other vibration consists of the carbon–oxygen bonds stretching out of phase with each other, resulting in a vibration where the carbon atom moves and the oxygen atoms do not. This out-of-phase vibration is an example of an antisymmetric vibration. In general, the antisymmetric vibration tends to be at higher frequency and the symmetric vibration tends to be at lower frequency than the natural frequency of the uncoupled oscillators.

Groups of atoms in a molecule that are not vibrationally coupled to the rest of the molecule, to a first approximation, have about the same frequencies of vibration in any molecule. This makes it possible to associate a vibrational frequency with a particular chemical functional group, such as a carbonyl group or a phenyl ring, without considering the rest of the molecule. These general-purpose vibrational frequencies are called group frequencies. Tabulations of group frequencies are typically refined to include the small frequency shifts caused by properties of the rest of the molecule, such as a weakening of the oscillator bond strength due to electron density withdrawal by the rest of the molecule. Tabulations of characteristic frequencies also are specific to a type of vibrational spectroscopy, since vibrations that produce a strong signal with one type may produce little or no signal with a different type of vibrational spectroscopy.

Molecular vibrations are often classified into groups that are intuitively descriptive of the vibrational motion. An oscillation in bond length is called a "stretch." An oscillation in bond angle is called a "deformation" or "bend." More specialized descriptions include terms such as "wag," "rock," or "breathing mode." Another way to classify molecular vibrations is by their symmetry properties using group theory. It can be shown that vibrations having certain symmetry properties will theoretically produce exactly zero signal for some types of spectroscopy, but not for other types of spectroscopy. Rules derived from symmetry considerations that identify vibrations expected to produce no spectroscopic signal are called selection rules. A detailed explanation of the use of group theory in vibrational spectroscopy is given in Refs 1 and 2.

1.3 INTERACTIONS BETWEEN ELECTROMAGNETIC RADIATION AND MATTER

1.3.1 Electromagnetic Radiation

Electromagnetic radiation consists of electric and magnetic fields oscillating in phase with each other and perpendicular to both each other and the direction of propagation. Gamma rays, X-rays, ultraviolet (UV) radiation, visible light, NIR and mid-IR radiation, terahertz (far-infrared) radiation, microwaves, and radio waves are all forms of electromagnetic radiation, differing only in their decreasing frequencies of oscillation. The energy of electromagnetic radiation is quantized. The smallest unit of light is the photon, having an energy, E, given by $E = h\upsilon$, where υ is the frequency of the electromagnetic radiation and h is Planck's constant.

Electromagnetic radiation can be thought of either as a particle (photon) or as a wave. We will use the representation that is most intuitive when describing phenomena involving electromagnetic radiation. For simplicity, we will use the term "light" as synonymous with electromagnetic radiation of any frequency, rather than just those frequencies that are visible to the human eye.

Light travels at 2.99792458×10^8 m/s in a vacuum. The speed of light can be used to convert time into distance, thereby providing depth resolution. Raman, mid-infrared, and near-infrared spectroscopies have all been used this way to make three-dimensional chemical images of objects in the atmosphere, such as clouds or discharge plumes.

Light of a particular frequency can be specified by its wavelength (the distance light travels during one oscillation cycle of the electric field), its wavenumber (the number of oscillating cycles per centimeter), or its energy (e.g., Joules per photon). For example, light having a frequency of 6.00×10^{14} Hz has a wavelength of 500 nm, a wavenumber of 20,000 cm^{-1}, and an energy of 3.98×10^{-19} J/photon, or 57.2 kcal/mol of photons.

Another important property of light is coherence. Coherence is a nonrandom relationship between photons. Coherence may be spatial (photon relationships based on photon location and/or direction) or temporal (relationships based on time when maxima in the oscillation fields of the photons occur). For example, a thermal light source is temporally incoherent because there is no mechanism coordinating the time that different photons are emitted. Lasers are temporally coherent because the process of stimulated emission causes the created photons to be in phase with the photons that stimulated the emission. Some spectroscopic processes such as coherent anti-Stokes Raman spectroscopy (CARS) or Raman gain spectroscopy rely on establishing temporal coherence between photons. Spectroscopic techniques such as FTIR (Fourier transform infrared spectroscopy) or OCT (optical coherence tomography) rely on establishing temporal coherence from nominally incoherent light sources.

1.3.2 Absorption and Emission of Light

A material having an internal process, such as molecular vibration, that is resonant with the frequency of incident light can be excited to a higher energy state by absorbing some of the light. The higher energy state usually relaxes back to the lowest energy state quickly by releasing heat and/or light. The strength of optical absorption or emission can be used to determine analyte concentration. Beer's law [3] relates analyte concentration to the strength of optical absorption, regardless of whether the transition involves an electronically, vibrationally, or rotationally excited state:

$$A_\lambda = -\log T = a_\lambda bc \tag{1.2}$$

where A_λ is the absorbance at wavelength λ, a_λ is the molar absorptivity at wavelength λ, b is the path length, c is the analyte concentration, and T is the transmittance, that is, ratio of transmitted intensity to incident intensity.

Emission intensity is also proportional to analyte concentration.

1.3.3 Refractive Index

Light slows down relative to its speed in a vacuum when traveling through matter. The ratio of the speed of light in a vacuum to that in a material is the refractive index of that material. Light incident on a planar interface between two transparent materials of different refractive indices is bent as a result of this speed change if the light is not perpendicular to the interface. The bending at this interface is described by Snell's law:

$$n_1 \sin\theta_1 = n_2 \sin\theta_2 \tag{1.3}$$

where n_1 is the refractive index of the first material, θ_1 is the angle of light with respect to interface normal in the first material, n_2 is the refractive index of the second material, and θ_2 is the angle of light with respect to interface normal in the second material.

The refractive index of a material changes with the wavelength of the light, as well as with the temperature of the material.

Light is also reflected at an interface between two transparent materials having different refractive indices. The reflected intensity is given by the Fresnel equations [4]

$$\begin{aligned} R_\perp &= \frac{I_R}{I_i} = \left(\frac{n_1\cos\theta_1 - n_2\cos\theta_2}{n_1\cos\theta_1 + n_2\cos\theta_2}\right)^2, \\ R_{//} &= \frac{I_R}{I_i} = \left(\frac{n_2\cos\theta_1 - n_1\cos\theta_2}{n_1\cos\theta_2 + n_2\cos\theta_1}\right)^2 \end{aligned} \tag{1.4}$$

where $R_\perp$ is the reflectance of light polarized perpendicular to the plane of incidence, $R_{//}$ is the reflectance of light polarized parallel to the plane of incidence, I_R is the intensity of reflected light, I_i is the intensity of incident light, n_1 is the refractive index of the first material, θ_1 is the angle of light with respect to interface normal in the first material, n_2 is the refractive index of the second material, and θ_2 is the angle of light with respect to interface normal in the second material.

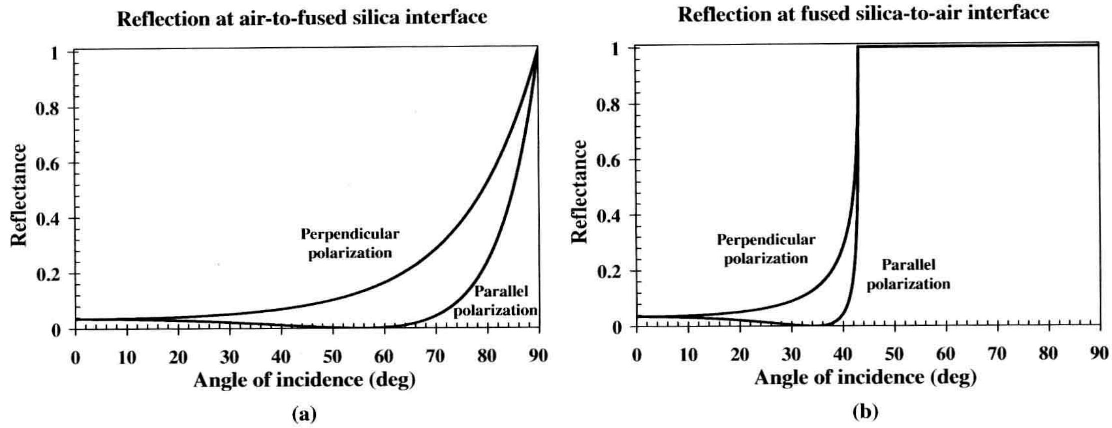

FIGURE 1.1 Fresnel reflection of 500 nm light at the interface between air and fused silica. (a) Light traveling from air into fused silica; (b) light traveling from fused silica into air.

Figure 1.1a and b shows the reflectivity of an interface between air ($n = 1.000$) and fused silica ($n = 1.462$) for both polarizations of 500 nm light. The reflectivity of the interface for light traveling into the higher refractive index material generally increases with angle of incidence, except for a reduction to zero at Brewster's angle θ_B ($\theta_B = \mathrm{Tan}^{-1}(n_2/n_1)$, or 55.6° in this example) for light polarized parallel to the plane of incidence. Light traveling from the higher index material experiences total internal reflection for incidence angles greater than the critical angle θ_c ($\theta_c = \mathrm{Sin}^{-1}(n_2/n_1)$, or 43.2° in this example). During total internal reflection, no energy is transmitted through the interface. An evanescent field does extend into the lower refractive index material, though. If a higher refractive index material, or an absorbing material, is placed in the evanescent field, energy can be transferred through the evanescent field to this material. The energy transfer process is called "attenuated total reflection" or ATR [5]. The evanescent field rapidly decays with distance from the interface:

$$d_p = \frac{\lambda}{2\pi n_1 (\sin^2 \phi - n_{21}^2)^{1/2}} \tag{1.5}$$

where d_p is the penetration depth of the evanescent field, λ is the wavelength of light, n_1 is the refractive index of the ATR crystal, ϕ is the internal angle of incidence, and n_{21} is the refractive index ratio of the sample to the ATR crystal.

ATR has an important role in some spectroscopic imaging techniques discussed later in this book.

As the dimensions of the refractive index interface approach the wavelength of light, diffraction effects dominate, and the interaction between light and the refractive index interface, which we now call a particle, is best described as Mie scattering. Mie scattered light travels in all directions from the particle. Most of the Mie scattered light intensity travels in the forward direction for particles 5–10 optical wavelengths in size. The scattered intensity becomes less directed as the particle size becomes smaller.

Molecules can scatter light in two different ways. If scattering does not change the energy of the light, it is called elastic scattering or Rayleigh scattering. Inelastic scattering or Raman scattering changes the energy of the scattered light. Raman scattering is described in greater detail later in this chapter. The intensity of molecular scattering is proportional to the fourth power of the optical frequency. Rayleigh scattering of polarized light is strongest in directions perpendicular to the electric field of the light and goes to zero in the direction parallel to the electric field. The polarization dependence of Raman scattered light is more complex and is described later in this chapter.

Light can be scattered many times when it interacts with a material consisting of a dense collection of many particles. The optical path through such a sample is best represented by a distribution of paths whose median can be 10–100 times longer than an unscattered path through the material. A large number of scattering events also tend to depolarize the light. Light that is ultimately reflected from a material after multiple scattering events is called diffusely reflected light. Similarly, light that is ultimately transmitted by a material after multiple scattering events is called diffusely transmitted light.

Diffuse reflectance and diffuse transmission usually degrade images. Spectroscopic imaging systems are often designed to minimize the detection of diffusely scattered light emanating from a sample. One exception is the use of spatially localized diffuse reflectance for depth discrimination and depth profiling. The most probable light paths through a highly scattering material form a banana-shaped volume connecting the point where light enters the material to a point where light exits the material, as illustrated in Figure 1.2. The depth of the material probed by the light increases with increasing separation of the optical entrance

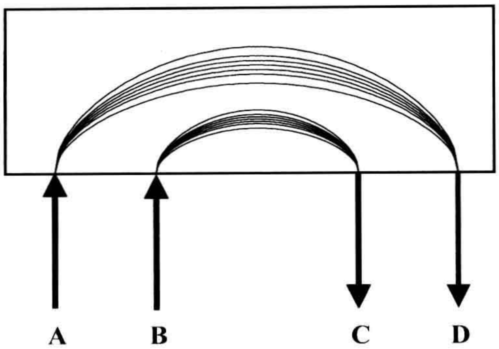

FIGURE 1.2 Depth discrimination in a highly scattering material by spatially resolved diffuse reflectance measurements. The most probable light paths connecting spatially separated excitation and collections points form a banana-shaped volume in the sample. Using points A and D for excitation and detection probes a greater depth than using points B and C for excitation and detection.

and exit points. This approach for depth discrimination and volume imaging has been extensively used in near-infrared spectroscopy [6–9]. Raman spectra have been collected this way through scattering media [10, 11], so perhaps Raman diffuse reflectance imaging is also possible.

1.3.4 Thermal Emission

All materials are continuously emitting radiation simply because they are at a temperature above absolute zero. If they are in equilibrium with their environment, they are also absorbing an equivalent amount of energy from the environment in order to maintain a constant temperature. A material that completely absorbs all frequencies of incident optical radiation, called an ideal blackbody source, has an emission spectrum given by [12]

$$H_\lambda(T) = \frac{2hc^2}{\lambda^5(e^{hc/\lambda kT}-1)}, \quad H_v(T) = \frac{2hc^2 v^3}{e^{hcv/kT}-1} \qquad (1.6)$$

where $H_\lambda(T)$ is the spectral radiant energy density per nanometer, $H_v(T)$ is the spectral radiant energy density per wavenumber, λ is the wavelength of light, v is the wavenumber of light, T is the temperature in Kelvin, h is Planck's constant (6.626×10^{-34} J s), c is the speed of light (2.998×10^8 m/s), and k is Boltzmann's constant (1.3807×10^{-23} J/K).

Real materials do not totally absorb all frequencies of electromagnetic radiation. Their emission spectra consist of an ideal blackbody emission spectrum multiplied by their absorbance spectrum, where absorbance is expressed as the fraction of light absorbed. For example, an ideal blackbody has a fractional absorbance of 1, and a completely transparent object has a fractional absorbance of 0.

Thermal emission spectroscopy can determine the absorption spectrum of a material from its spontaneous emission of light. Laboratory samples are often heated to improve the quality of the data. Chemical imaging based on thermal emission spectroscopy is extensively used for remote sensing, which is described in more detail at the end of this chapter.

1.3.5 Fluorescence

Fluorescence is one process where an electronically excited state decays to a lower electronic state by emitting a photon. An energy level diagram describing fluorescence is shown in Figure 1.3. The excited state is usually the lowest vibrational level of the first excited singlet electronic state. The lower state is usually one of many vibrational levels in the electronic ground state. The emission bands to the vibrational levels in the ground state overlap spectrally giving a relatively broad fluorescence emission spectrum with few spectral features.

The lifetime of the fluorescence process is typically on the order of 1–10 ns. Kinetically competing processes that return a molecule from the electronic excited state to the ground state without the emission of a photon, called dark reactions, reduce the fluorescence lifetime. They also reduce the fluorescence quantum yield, defined as the number of fluorescence photons produced divided by the number of molecules in an excited state capable of producing fluorescence photons. The process of reducing the fluorescence quantum yield is called fluorescence quenching. Highly fluorescent molecules have quantum yields very close to 1.

Absorption of a photon is the most common mechanism for creating the excited state necessary for fluorescence emission. Other mechanisms include chemical excitation

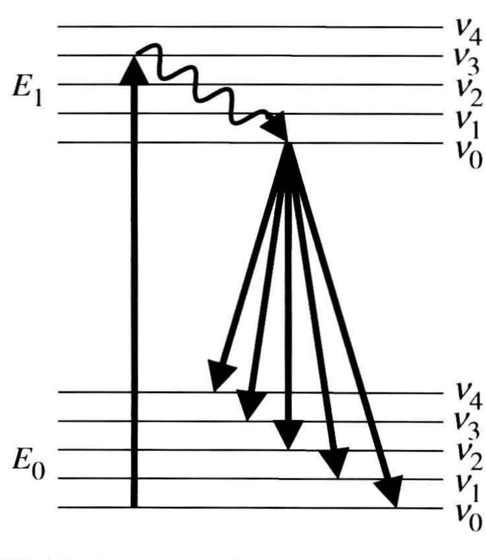

FIGURE 1.3 Energy level diagram illustrating fluorescence.

(chemiluminescence) or electron bombardment (cathodoluminescence). The absorption spectrum for the process of creating excited states for fluorescence emission is called the fluorescence excitation spectrum. The absorption spectrum of a material is the sum of the fluorescence excitation spectrum and the absorption spectrum of all processes that do not produce fluorescence. Materials having a single fluorescent species have the same emission spectrum at all excitation wavelengths, since fluorescence almost always occurs from the lowest vibrational level of the first electronic excited state, regardless of how that state got populated.

The fluorescence emission spectrum from impurities is often the combined spectra of many different chemical compounds. The observed fluorescence therefore has properties that differ from the fluorescence of a pure material. Excitation and emission spectra may be spectrally broader. The shape of the emission spectrum may change significantly with changing excitation wavelength, or during fluorescence quenching. The fluorescence decay rate may become very nonexponential due to different impurity fluorescence lifetimes. Since materials having multiple fluorescent species can have multiple excitation spectra, excitation–emission matrices are used to describe their fluorescence. Excitation–emission matrices are three-dimensional plots on axes of excitation wavelength, emission wavelength, and emission intensity.

Fluorescence imaging is a powerful and very popular chemical imaging technique, but it is outside the scope of this book. We include fluorescence here because it is often a serious nuisance that limits the capabilities of Raman chemical imaging. This limitation will be discussed in greater detail later in the book. In the context of Raman spectroscopy, the term fluorescence is often used generically to mean any process (often unknown) that produces a spectrally broad background intensity. Phosphorescence is one example of a nonfluorescence process that may be mistaken for fluorescence in a Raman measurement.

TABLE 1.1 Mid-Infrared Characteristic Frequencies for Several Common Functional Groups

Vibration	Shift (cm^{-1})	Group
OH stretch (dilute solution)	3600–3700	–OH in alcohols and phenols
OH stretch (solids and liquids)	3250–3420	–OH in alcohols and phenols
NH_2 antisymmetric stretch (solids)	3340–3360	–NH_2 in primary amines
H-bonded OH stretch; very broad	2400–3100	–OH in carboxylic acids
=C–H stretch	3000–3100	Unsaturated hydrocarbons
C–H stretch	2850–2990	Aliphatic hydrocarbons
C≡N stretch	2200–2260	Nitriles
Overtones and combination bands	1650–2000	Substituted benzene rings
C=O stretch	1650–1870	Carbonyl compounds
C=O stretch	1740–1750	Esters
C=O stretch	1700–1720	Ketones
NH_2 deformation	1580–1650	Primary amines
Ring stretch, sharp peak	1590–1615	Benzene ring in aromatics
COO^- antisymmetric stretch	1560–1610	Carboxylic acid salts
Antisymmetric CH_3 deformation	1440–1465	CH_3 in aliphatics
Symmetric CH_3 deformation	1370–1380	CH_3 in aliphatics
C–O stretch	1015–1200	Alcohols
Si–O–Si antisymmetric stretch	1000–1100	Siloxanes
C–Br stretch	500–650	C-Br in bromo compounds
COC bend	430–520	Ethers
CNC bend	400–510	Amines

Compiled from Ref. 15.

1.4 MID-INFRARED ABSORPTION SPECTROSCOPY

The mid-infrared spectral range includes wavelengths from about 2.5 to 25 μm. This corresponds to about 4000–400 cm^{-1} or 11–1.1 kcal/mol. Absorption in this spectral region is due to molecular vibrations that modulate the dipole moment of the molecule. The energy of these vibrations is small compared to the energy of a chemical bond. For example, the C–H bond energy of 98 kcal/mol is 12 times greater than the vibrational energy, 8.4 kcal/mol, of the C–H stretching vibration at 2950 cm^{-1}.

Table 1.1 lists some characteristic mid-infrared absorption frequencies of common functional groups. Much more extensive tables are given in Refs 13–15. Tables such as these provide a good starting point for estimating the spectral location of mid-infrared absorption bands that may be analytically useful for chemical imaging. They are also useful for assigning bands observed in a spectrum of a known material to chemical groups in the material.

Huge libraries of mid-infrared spectra are available that can provide the experimentally observed spectrum of most common materials, often eliminating the need to estimate spectra from characteristic frequency tables. These commercial libraries can be supplemented by custom libraries or small sets of experimental spectra collected from standards. When the spectrum of a desired material is not available from libraries, the spectra of several related materials from the library can be used as a highly specific characteristic frequency table to estimate the desired spectrum.

TABLE 1.2 Mid-Infrared Molar Absorptivities for Several Common Functional Groups

Band Descripton	Sample	Band Position (cm^{-1})	Molar Absorptivity (L/(mole cm))	Path Length for 1 AU in Neat Material (μm)
OH stretch	Water	3404	100	1.8
OH bend	Water	1643	22	8.3
CH stretch	Toluene	3025	53	20.2
CH bend	Toluene	728	302	3.5
Ring stretch	Toluene	1496	94	11.4
CH bend	Dichloromethane	1265	109	5.9
CH stretch	Dichloromethane	3054	8	83.1
CH stretch	Benzene, 25°C	3036	79	11.2
CH bend	Benzene, 25°C	673	397	2.2
Ring stretch	Benzene, 25°C	1478	102	8.7
CH stretch	Acetonitrile	2944	5.83	90.5
CH bend	Acetonitrile	1445	15.54	34.0

Compiled from Refs 16–20.

The intensity of mid-infrared absorption by a molecular vibration is proportional to the square of the change in dipole moment. Functional group absorptivities are not as generally useful as functional group frequencies, however, because dipole moments are much more sensitive to neighboring group effects. The absorptivities of molecular vibrations do follow Beer's law, however, so mid-infrared molar absorptivities are useful for measuring analyte concentrations. Table 1.2 lists reported molar absorptivities for vibrations in some common materials. The relatively strong mid-infrared absorption of these materials requires sample path lengths to be on the order of 10 μm or less to yield undistorted spectra.

Not all molecular vibrations absorb light. For example, the symmetric stretching vibration of carbon dioxide described earlier has the changing dipole moment of one C–O bond exactly cancelled out by the changing dipole moment of the other C–O bond. Since this vibration has zero change in its dipole moment, it cannot absorb infrared light. More generally, group theory can be used to identify vibrations having a symmetry that causes any change in the dipole moment of one chemical bond to be cancelled by a corresponding change in another chemical bond. Such vibrations do not absorb light, and are called symmetry forbidden.

Mid-infrared absorption chemical images can be created by measuring spectra of external light intensity *not* absorbed by the sample. Three different techniques to do this are based on measuring light intensity after transmission through the sample, after reflectance from the sample, and after ATR. All three techniques can produce images by mapping or by global imaging. ATR can be used in a different mode to measure mid-infrared depth profiles by changing the penetration depth of the evanescent wave [21]. This can be done by varying the angle of incidence at the point of total internal reflection or by using ATR elements having different refractive indices.

Mid-infrared depth profiles can also be created by measuring the light intensity absorbed by a material using photoacoustic spectroscopy [22]. Absorbed light produces a thermal wave that travels back to the surface of the sample. Some of the thermal wave energy couples into gas at the sample interface producing sound that is detected by a sensitive microphone. The penetration depth into the sample is determined by the modulation frequency of the mid-infrared light, which can be changed by changing the scan speed of a Fourier transform mid-infrared instrument. Sampling depths typically range from several to 100 μm.

Mid-infrared chemical images can be created from the spontaneous thermal emission spectra of objects as well, since an object's absorption spectrum can be deduced from its emission spectrum. Between -20 and $+50$ °C, typical of environmental temperatures on the Earth, the wavelength of maximum ideal blackbody intensity is between 9 and 11.5 μm. These emission wavelengths are not only in the center of the highly predictive mid-infrared fingerprint spectral region, but also in the atmospheric transmission window between 8 and 14 μm. This makes mid-infrared emission spectroscopy especially attractive for remote sensing. Laboratory applications of mid-infrared emission spectroscopy often involve sample heating, since sensitivity increases with increasing temperature difference between the sample and the detector.

1.5 FAR-INFRARED AND TERAHERTZ SPECTROSCOPY

The far-infrared, terahertz, and submillimeter spectral regions are all labels for approximately the same interval in the electromagnetic spectrum. This spectral interval includes wavelengths ranging from about 25 to 1000 μm. This corresponds to about 400–10 cm^{-1}, 12–0.3 THz, or 1.14–0.0286 kcal/mol. Room-temperature thermal energy,

kT, is in this spectral range at about 207 cm^{-1}. The different names, and differing spectral limits for the region, have been associated with different bodies of experimental technique. Both "far-infrared" and "submillimeter" imaging and spectroscopy are copious in the astronomical and remote sensing literature. "Terahertz" has become more often associated with measurements in this spectral region using innovative new light sources and detection methods based on femtosecond lasers, quantum cascade lasers, or nonlinear optical techniques.

Light absorption in the far-infrared region requires dipole moment oscillation at lower frequencies than in the mid-infrared spectral region, implying harmonic oscillators with greater masses and/or weaker bond strengths. Intramolecular vibrations contributing to this spectral region include stretching of bonds involving heavy atoms, organic skeletal bending modes, torsional modes (restricted rotational motion about single bonds), and ring puckering of small-ring molecules. Intermolecular vibrations, between different molecules associated by hydrogen bonding or electrostatic interactions, also occur in this spectral region, as well as crystal lattice modes of polymers and inorganic solids. Pure rotational transitions of light, gas-phase molecules extend from the microwave region into the far-infrared region. Table 1.3 gives some typical molar absorptivities for some far-infrared absorption bands.

Blackbody excitation sources for spectroscopy are very weak in the far-infrared spectral region. While other light sources such as the HCN laser, quantum cascade lasers, and difference-frequency generation optics are available for making traditional transmission measurements in this spectral region, terahertz spectroscopy [27] has arisen as the primary far-infrared imaging technology. Terahertz spectroscopy uses unique light sources and detection methods that give it capabilities not available to traditional absorption spectroscopy. Briefly, pulses of terahertz radiation are generated by illuminating a biased photoconductive antenna with ultrashort pulses of near-infrared light from a titanium sapphire laser. The pulses are detected with a similar time-gated photoconductive antenna. The transit time, phase, and amplitude of the subpicosecond terahertz pulse are recorded after it interacts with the sample, making possible the calculation of distance and both the refractive index and absorption spectrum of the sample.

Terahertz instruments are usually operated in either an imaging mode or a spectroscopic mode, though combination 3D spectroscopic imaging devices have been reported [28]. The imaging mode measures the reflections from the sample that occur at interfaces between compositions of differing refractive index. The refractive indices of the materials in adjacent layers are determined from the intensity of the reflection using the Fresnel equations. The thickness of a layer is determined from the time between reflections from the interfaces at the start and end of the layer. Each pixel in a two-dimensional map can provide a depth profile of the sample refractive index. A three-dimensional map of an entire pharmaceutical tablet can be collected in several minutes. The lateral spatial resolution is diffraction limited at hundreds of micrometers, while the axial resolution is determined by the instrument time resolution, which is usually on the order of 30 μm.

TABLE 1.3 Far-Infrared Molar Absorptivities for Some Common Materials

Sample	Spectral Position (cm^{-1})	Molar Absorptivity (L/(mole cm))	Path Length for 1 AU in Neat Material (mm)
Benzene	300	0.110	8.1
Benzene	185	180	0.005
Benzene	33[a]	0.24	3.7
Toluene	345	1.63	0.66
Toluene	33[a]	0.5	2.1
Dichloromethane	285	2.77	0.23
Methanol	34[a]	2.22	0.18
Water	198	9.35	0.019
Water	32[a]	1.82	0.10
Hexane	33[a]	0.09	15

Compiled from Refs 20 and 23–26.

[a] Slowly varying background absorption, not a peak location.

The spectroscopic mode of a terahertz instrument can determine the absorption spectrum of a sample by Fourier transforming a terahertz pulse transmitted by the sample. The use of transmission rather than reflection eliminates spectral artifacts that would result from including pulse reflection in the Fourier transformation. Spectra of individual layers can be obtained, however, by using a windowed Fourier transform between reflected pulses when carrying out terahertz imaging. The quality of these spectra may be compromised, by refractive index heterogeneity in the layer.

Far-infrared emission spectroscopy is extensively used for making chemical images of deep space. This topic will be covered in greater detail in Section 1.8.

1.6 NEAR-INFRARED ABSORPTION SPECTROSCOPY

The near-infrared spectral range includes wavelengths from about 0.78 to 2.5 μm. This corresponds to about 12,820–4000 cm^{-1} or 37–11 kcal/mol. The energies of these vibrations are greater than those of the mid-infrared fundamental vibrations, but still considerably less than the bond energies of the vibrating chemical bonds. For example, the C–H bond energy of 98 kcal/mol is 5.8 times greater than the 5870 cm^{-1} C–H stretching vibration's first overtone energy of 16.8 kcal/mol.

Absorption in this spectral region is due to overtone and combination bands of molecular vibrations that modulate the dipole moment of the molecule. Overtone bands result from